TEMPORAL SHAPING OF SIMULATED TIME SERIES WITH CYCLICAL SAMPLE PATHS

WEIWEI CHEN

Department of Supply Chain Management, Rutgers University, Rutgers Business School – Newark and New Brunswick, 1 Washington Park, Newark, NJ 07901, USA
E-mail: wchen@business.rutgers.edu

ALOK BAVEJA AND BENJAMIN MELAMED

Department of Supply Chain Management, Rutgers University, Rutgers Business School – Newark and New Brunswick, 100 Rockafeller Road, Piscataway, NJ 08854, USA
E-mail: baveja@business.rutgers.edu; melamed@business.rutgers.edu

Temporal shaping of time series is the activity of deriving a time series model with a prescribed marginal distribution and some sample path characteristics. Starting with an empirical sample path, one often computes from it an empirical histogram (a step-function density) and empirical autocorrelation function. The corresponding cumulative distribution function is piecewise linear, and so is the inverse distribution function. The so-called inversion method uses the latter to generate the corresponding distribution from a uniform random variable on [0,1), histograms being a special case. This paper shows how to manipulate the inverse histogram and an underlying marginally uniform process, so as to "shape" the model sample paths in an attempt to match the qualitative nature of the empirical sample paths, while maintaining a guaranteed match of the empirical marginal distribution. It proposes a new approach to temporal shaping of time series and identifies a number of operations on a piecewise-linear inverse histogram function, which leave the marginal distribution invariant. For cyclical processes with a prescribed marginal distribution and a prescribed cycle profile, one can also use these transformations to generate sample paths which "conform" to the profile. This approach also improves the ability to approximate the empirical autocorrelation function.

Keywords: ARM processes, autocorrelation functions, histograms, model fitting, modeling time series, temporal shaping, TES processes

1. INTRODUCTION

Consider an empirical time series, $\{Y_n\}_{n=0}^{N}$, assumed to be from a stationary probability law. Suppose we calculate from $\{Y_n\}$ its empirical (histogram) probability density function (pdf), $\hat{h}_Y(y)$, and the corresponding empirical cumulative distribution function (cdf), $\hat{H}_Y(y)$, as well as the corresponding empirical autocorrelation function, $\hat{\rho}_Y(\tau)$. Thus, we estimate first-order and second-order statistics of the empirical data, the latter capturing

information on temporal dependence in the empirical sequence, $\{Y_n\}$. The general problem is to construct a time series model, $\{X_n\}$, whose marginal cdf, F_X, approximates $\hat{H}_Y$, and whose autocorrelation function, $\rho_X(\tau)$, approximates $\hat{\rho}_Y(\tau)$.

A popular method for generating variates from a prescribed distribution, F, is the *inversion method* (see Bratley, Fox, and Schrage [2]). If U is a random variable uniformly distributed over [0,1), then the random variable $X = F^{-1}(U)$ has distribution F (denoted $X \sim F$). One approach to fitting a model to the pair $(\hat{h}_Y, \hat{\rho}_Y)$ is given in Liu and Munson [6]. The idea is to construct a filter (an autoregressive scheme) for independent and identically distributed (i.i.d.) normal sequence $\{Z_n\}$, thereby producing an autocorrelated normal sequence $\{B_n\}$, called the *background sequence*. A transformation $D = F^{-1} \circ G$, called a *distortion*, is applied to each B_n, where G is the marginal normal distribution of the B_n, so $G(B_n) \sim \text{Uniform}(0, 1)$, and F^{-1} is the inverse distribution function of interest (in our case it corresponds to the observed inverse histogram, $\hat{H}_Y^{-1}$). The resulting sequence $X_n = D(B_n)$, called the *foreground sequence*, then models the observed data. In particular, the inversion method guarantees that $\{X_n\}$ has the prescribed marginal distribution, F. The problem is to design the filter, so as to approximate the observed $(\hat{H}_Y, \hat{\rho}_Y)$. A related approach appears in Cario and Nelson [3,4], which starts with a marginally normal random sequence, and then transforms it into any marginal distribution and approximate autocorrelation function.

The approach we take here is related to Liu and Munson [6], but with some modifications. First, we would like the background sequence $\{B_n\}$ to be an autocorrelated identically distributed Uniform (0,1) sequence $\{U_n\}$, so the distortion D often reduces to F^{-1}; and second, $\{Z_n\}$ is an i.i.d. Uniform (0,1) pseudo-random number stream, available on most computers. Examples of such approaches are generation methods based on Transform-Expand-Sample (TES) processes (see Melamed [14]; Jagerman and Melamed [8,9]), and Auto-Regressive Modular (ARM) processes (see Melamed [16]) – a generalization of TES processes, as well as Minification/Maxification methods (see Lewis and McKenzie [7]). This paper is based on ARM processes, to be briefly reviewed in Section 3. We mention that search algorithms have been developed for fitting ARM processes to a prescribed pair consisting of a marginal distribution and autocorrelation function. More specifically, given such a pair, the algorithm searches for an ARM process that fits exactly the prescribed marginal distribution and simultaneously approximates the prescribed autocorrelation functions (Jagerman and Melamed [11]; Jelenkovic and Melamed [12,13]).

In this paper, we observe that the inverse histogram and the background uniform process may be manipulated so as to "shape" model sample paths in a controlled way. The goal is to find a stationary model, which preserves the empirical marginal distribution, approximates the empirical autocorrelation function, and gives rise to model sample paths that qualitatively "resemble" the empirical data, all the while retaining an exact match to the (prescribed) empirical distribution. To this end, we propose a new approach to temporal shaping of time series, to be defined in Section 4. Specifically, we identify a number of operations on a piecewise-linear inverse distribution function, which leave the marginal distribution invariant. For cyclical processes with a prescribed marginal distribution and a prescribed cycle profile, one can also use these transformations to generate sample paths, which "conform" to the prescribed profile. Overall, given a histogram marginal distribution and autocorrelation function, our shaping procedure consists of two steps: first, the corresponding linear inverse distribution function is transformed to approximate the prescribed profile using a heuristic procedure (see Section 5.1); and second, a proposed search algorithm uses the approximate profile and prescribed autocorrelation function to fit an ARM process to them (see Section 5.2).

Henceforth, we restrict the discussion to the case where the sample paths have an apparent cyclical structure, but otherwise, cycle lengths and histories are random. Unless otherwise specified, a distortion D is a measurable function on the interval $[0, 1)$.

The remainder of this paper is organized as follows. Section 2 provides some background material on histogram distributions. Section 3 provides technical preliminaries on ARM processes and the notion of pseudo-time. Section 4 describes a set of distribution-invariant operators, while Section 5 proposes a heuristic for temporal shaping of cyclic ARM time series. Finally, Section 6 concludes the paper.

2. VARIATES WITH HISTOGRAM DENSITIES

Suppose that the empirical distribution is modeled by a histogram $\hat{\mathcal{H}}_Y$, specified as a finite set of triplets

$$\hat{\mathcal{H}}_Y = \{(l_j, r_j, \hat{p}_j) : 1 \leq j \leq J\}, \tag{1}$$

where J is the number of histogram cells, $[l_j, r_j)$ is the interval of cell j, and $\hat{p}_j$ is the probability estimator of cell j. We assume, for simplicity, that cell intervals are sorted in increasing order and disjoint (i.e., $[l_i, r_i) \cap [l_j, r_j) = \emptyset, i \neq j$), and that the index set $\mathcal{I} = \{1, \ldots, J\}$ of histogram cells already reflects this ordering. Recall that the parameters J and the intervals $[l_j, r_j), 1 \leq j \leq J$, are prescribed and used to calculate the $\hat{p}_j$ from $\{Y_n\}$ as relative frequencies. Define the index set $\mathcal{I}^+ = \{j \in \mathcal{I} : \hat{p}_j > 0\}$. The histogram $\hat{\mathcal{H}}_Y$ induces the (step-function) empirical density,

$$\hat{h}_Y(y) = \sum_{j \in \mathcal{I}^+} 1_{[l_j, r_j)}(y) \frac{\hat{p}_j}{w_j}, \quad -\infty < y < \infty, \tag{2}$$

where $1_A(x)$ is the indicator function of set A, and $w_j = r_j - l_j > 0$ is the width of cell j. Thus, the empirical density $\hat{h}_Y(y)$ is a probabilistic mixture of uniform densities over the intervals $[l_j, r_j)$ with mixing probabilities $\hat{p}_j$. Note that the cell widths, w_j, in Eq. (2) are cell dependent. Further, assuming that the cells are contiguous, we shall simplify the notation by denoting the end points of the cells by $s_0, s_1, \ldots, s_{J+1}$, so that step supports have the form $[l_j, r_j) = [s_{j-1}, s_j)$, for all $1 \leq j \leq J$. We will show at the end of this section that this assumption does not invalidate the discussion to follow. A simple example of a histogram pdf, $\hat{h}_Y$, is depicted in Figure 1.

Clearly, the probability that an empirical observation falls in the range $[s_{j-1}, s_j)$ is just the area of cell j; the area under the function $\hat{h}_Y$ is, of course, 1. The cdf $\hat{H}_Y$, corresponding to the histogram pdf, $\hat{h}_Y$, is the piecewise-linear function

$$\hat{H}_Y(y) = \begin{cases} 0, & y < s_0, \\ \hat{C}_{j-1} + (y - s_{j-1})\dfrac{\hat{p}_j}{w_j}, & y \in [s_{j-1}, s_j), 1 \leq j \leq J, \\ 1, & y \geq s_J, \end{cases} \tag{3}$$

where $\{\hat{C}_j\}_{j=0}^J$ is the cdf corresponding to $\{\hat{p}_j\}_{j=1}^J$, given by

$$\hat{C}_j = \begin{cases} 0, & j = 0, \\ \displaystyle\sum_{i=1}^j \hat{p}_i, & 0 < j < J, \\ 1, & j = J. \end{cases} \tag{4}$$
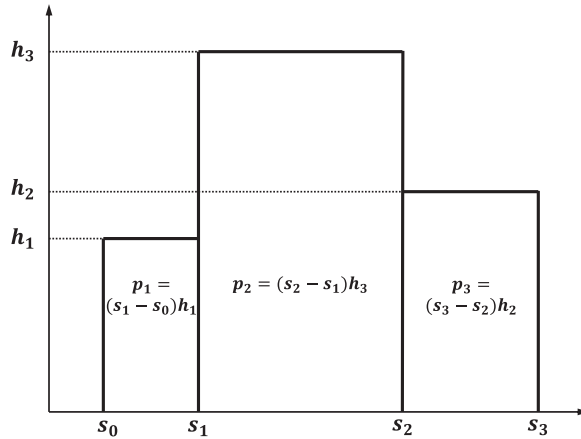
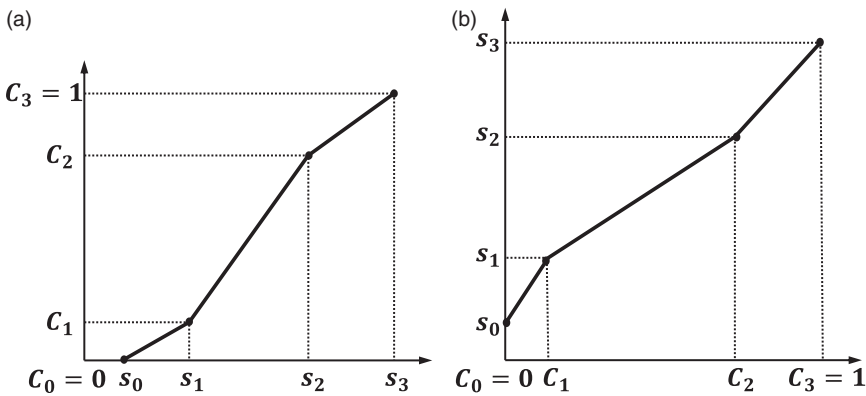FIGURE 1. Histogram pdf, $\hat{h}_Y$.

FIGURE 2. Histogram cdf (left) and inverse histogram cdf (right), corresponding to the histogram pdf, $\hat{h}_Y$. (a) Histogram cdf, $\hat{H}_Y$. (b) Inverse histogram cdf, $\hat{H}_Y^{-1}$.

Since $\hat{H}_Y$ is a piecewise-linear function, so is its inverse, $\hat{H}_Y^{-1}$. The latter is given by

$$\hat{H}_Y^{-1}(x) = \sum_{j \in \mathcal{I}^+} 1_{[\hat{C}_{j-1}, \hat{C}_j)}(x) \left[s_{j-1} + (x - \hat{C}_{j-1}) \frac{w_j}{\hat{p}_j} \right], \quad 0 \le x \le 1. \tag{5}$$

Figure 2 depicts the histogram cdf, $\hat{H}_Y$, and its inverse, $\hat{H}_Y^{-1}$, corresponding to the histogram density, $\hat{h}_Y$, of Figure 1.

In order to use the inversion method for generating a Monte Carlo time series with marginal density $\hat{h}_Y$, we employ the distortion $D = \hat{H}_Y^{-1}$. Operationally, this can be described by the following random experiment:

1. Sample a number u from the Uniform $(0,1)$ distribution.
2. Find the index j such that $\hat{C}_{j-1} \le u < \hat{C}_j$.
3. Return $x = s_{j-1} + (u - \hat{C}_{j-1}) \frac{w_j}{\hat{p}_j}$.

The corresponding output random variable, X, has the requisite distribution, $\hat{h}_Y$. Note that even if steps are not contiguous (see our assumption made at the beginning of this session),

Eqs. ([3](#))–([5](#)) and the above procedure are still valid by simply replacing s_{j-1} with l_j and s_j with r_j for $j \in \mathcal{I}^+$. Hence, for simplicity, the discussion to follow will assume that the steps are contiguous with $[l_j, r_j) = [s_{j-1}, s_j)$.

3. THE NOTION OF PSEUDO-TIME

Suppose that a stationary sequence $\{U_n\}$ has been generated from a Uniform (0,1) distribution, and that each U_n has been transformed into the corresponding X_n by some distortion $D(U_n) = X_n$. If $\{U_n\}$ is cyclical in structure, then one way to view it is as a random process on the circular unit interval (i.e., a unit circle with circumference 1) with net clockwise drift. Recall that the unit circle with circumference 1 is a geometric model of modulo-1 arithmetic, where the modulo-1 operator $\langle \cdot \rangle$ (fractional part) is defined by $\langle x \rangle = x - \lfloor x \rfloor$ where $\lfloor \cdot \rfloor$ is the floor operator; see for example, Jagerman and Melamed [8]. As $\{U_n\}$ sweeps the abscissa in the domain $[0, 1)$ of D from left to right, the transformed values $\{X_n\}$ will roughly follow the outline of the curve D. Eventually, the $\{U_n\}$ will wrap-around from a neighborhood of the point 1 to a neighborhood of the point 0, and a new "cycle" will begin. This behavior manifests itself in the sample paths as visually distinct blocks (cycles), especially when the leading autocorrelations of $\{U_n\}$ are of high magnitude. Of course, a mathematical device, such as spectral analysis, can aid the "naked eye" in identifying "random" periodicities, whereas periodogram analysis can aid in finding deterministic ones. Intuitively, a cycle's profile ("average envelope") will roughly follow the shape of curve D, and the more so if the drift is pronounced, that is, when the next point lies, say, "clockwise" relative to the previous one on the unit circle, with high probability. Note that for the distortion and profile to be comparable, the profile domain need to be scaled to the domain of D, namely, to the interval $[0,1)$. To this end, letting $\varphi(n), n = 0, \ldots, N - 1$, be the cycle profile, where N is the period, the normalized cycle profile is given by

$$\tilde{p}\left(\frac{n}{N}\right) = \varphi(n), \quad n = 0, \ldots, N - 1. \tag{6}$$

To fix the ideas, consider the class of so-called ARM^+ *background* processes (Jagerman and Melamed [8–10]; Melamed [16]) of the form

$$U_n^+ = \langle U_{n-1}^+ + V_n \rangle, \tag{7}$$

where $U_0^+ \sim \text{Uniform}(0, 1)$ and the sequence $\{V_n\}_{n=1}^{\infty}$, called the *innovation* sequence, is independent of U_0^+, with marginal density f_V. Lemma 1 below states the known result that uniformity is closed under modulo-1 addition of independent random variables.

LEMMA 1 (Feller [5], p. 64): *Let $U \sim \text{Uniform}(0, 1)$ and let V be any random variable independent of U. Then, one has $W = \langle U + V \rangle \sim \text{Uniform}(0, 1)$.*

Lemma 1 guarantees that the ARM^+ background sequence $\{U_n^+\}$ is marginally uniform on $[0, 1)$, and hence its corresponding foreground sequence, $\{X_n\}$, generated by the distortion $D = \hat{H}_Y^{-1}$ as $X_n = \hat{H}_Y^{-1}(U_n^+)$ has marginal cdf $\hat{H}_Y$. We mention that in order to fit a general ARM process to a prescribed distribution and autocorrelation function simultaneously, a heuristic search is performed to identify a suitable innovation density that results in a foreground (ARM) sequence that approximates the prescribed autocorrelation, while the prescribed distribution is reproduced exactly by virtue of the inversion method (see Melamed [16]).

To simplify the discussion, we focus on *basic ARM$^+$* processes – those with uniform innovations of the form

$$V_n \sim \mathrm{Uniform}(L, R), \tag{8}$$

parameterized by pairs (L, R), subject to $-0.5 \leq L < R < 0.5$. The cyclical structure of $\{U_n^+\}$ is better expressed under the alternate equivalent parameterization (α, ϕ), where $\alpha = R - L$ and $\phi = (R + L)/\alpha$. More specifically $\phi \neq 0$ corresponds to drift, and $\phi = 0$ corresponds to no drift; the higher $|\phi|$, the more pronounced the drift. When $\phi = 0$, the entire data set corresponds to one (infinite) cycle, and so cyclical structure is not apparent. The parameter α has a strong effect on the autocorrelations of $\{U_n^+\}$; the smaller α, the higher the autocorrelations. See Melamed [15] for more details.

The discussion above motivates the view of a background sequence, $\{U_n\}$, as a "pseudo-time" (within cycles). While normal time advances uniformly (at rate 1) and monotonically, a pseudo-time $\{U_n\}$ advances only on average by virtue of its drift. Since we deal with a discrete time random process, the increments, $U_{n+1} - U_n$, are generally random and may even be negative. Nevertheless, the existence of drift allows us to think of $\{U_n\}$ as pseudo-time (actually a metaphor for time), this term merely serving as a convenient figure of speech. Certainly, the background variates U_n affect the behavior of the corresponding foreground variates $X_n = D(U_n)$ within cycles, in that they determine the (random) cycle length, whereas D controls the temporal behavior (profile) of the X_n.

4. TEMPORAL SHAPING OPERATIONS

The term *temporal shaping* is used in this paper to refer to the collective activities of manipulating the distortion, D, in a model of the form $X_n = D(U_n)$, so as to engender simulated sample paths which conform to or approximate a prescribed cycle profile, but are subject to the constraint that the observed histogram, $\hat{\mathcal{H}}_Y$, is preserved by the model. Naturally, this activity will tend to improve the fit of the model autocorrelation function, ρ_Y, to its empirical counterpart, $\hat{\rho}_Y$, because temporal shaping *ipso facto* gives rise to sample paths that better resemble their counterparts in the empirical time series.

In our case, temporal shaping consists of replacing the inversion distortion, $\hat{H}_Y^{-1}$, by a new distortion, D, such that $D(U) \sim \hat{H}_Y$; here D is a general distortion, not necessarily monotone, so that the inversion method is not used *per se*; rather, a more general analog is employed. The idea is that the cycle profile can be approximated by $\hat{H}_Y$-invariant operations on the original distortion $\hat{H}_Y^{-1}$, because distortions can be thought of as defining a cycle profile, particularly when driven by a highly autocorrelated, marginally Uniform (0,1) process with positive drift on the unit circle. Recall that as the uniform process sweeps the interval $[0, 1)$ from left to right, the resulting D-transformed values roughly follow the outline of D.

We now turn to identifying temporal shaping operations with the requisite properties. Such operations are generally distribution preserving. However, we distinguish between operations on the background uniform sequence, $\{U_n\}$, called *pre-distortion transformations*, and operations on the inverse histogram distortion, $\hat{H}_Y^{-1}$, called *distribution-invariant operators*. Pre-distortion transformations are uniformity-preserving mappings from $[0, 1)$ to itself; as such, they map one uniform background process to another. Consequently, a distortion transformation may follow a pre-distortion transformation to achieve the desired marginal distribution. Distribution-invariant operators modify a histogram $\hat{H}_Y^{-1}$, replacing it by a piecewise-linear distortion, not necessarily monotone. Temporal shaping operations will be discussed next in some detail.

4.1. Stitching Transformations

The family of so-called stitching transformations, S_ξ, $0 \leq \xi \leq 1$, is a class of pre-distortion transformations (in our case, pre-inversion transformations), given by

$$S_\xi(y) = \begin{cases} \dfrac{y}{\xi}, & 0 \leq y \leq \xi, \\[2mm] \dfrac{1-y}{1-\xi}, & \xi \leq y \leq 1. \end{cases} \tag{9}$$

A picture of some typical stitching transformations appears in Figure 3. Clearly, S_1 is the identity ($S_1(y) = y$), and S_0 is the antithetic (reflection) transformation ($S_0(y) = 1 - y$). For $0 < \xi < 1$, S_ξ has a "triangular" appearance; for this reason, they are also called *tent transformations*. When applied to a cycle of an ARM$^+$ sequence, its effect is to skew the cycle into some profile from Figure 3. In other words, for a cycle length c, the sequence $\{S_\xi(U_n)\}$ will peak at the point ξc. Thus, as ξ varies from 0 to 1, the profile changes continuously from the antithetic form ($\xi = 0$) to a tent form ($0 < \xi < 1$), finally becoming the identity ($\xi = 1$). Since ξ is the fraction of the cycle where the peak occurs, changing ξ leads to a continuum of correspondingly skewed sample path cycles.

The merit of the S_ξ lies in the fact that if $U \sim$ Uniform $(0, 1)$, then $S_\xi(U) \sim$ Uniform $(0, 1)$ for all $0 \leq \xi \leq 1$ (see Lemma 2 of Melamed [14]). Thus, not only can stitching transformations shape marginally uniform sample paths (by skewing), they also preserve their marginal uniformity, thereby allowing us to apply further distortions.

Suppose that $\{U_n\}$ is a positively autocorrelated uniform background sequence, and we use S_ξ as a pre-inversion, followed by some distortion D. Define the composite distortion, $D_\xi = D \circ S_\xi$, for some $0 \leq \xi \leq 1$. In particular, taking $D = \hat{H}_Y^{-1}$ gives rise to composite distortions, $D_{Y,\xi}$, such that for each $0 \leq \xi \leq 1$, the foreground variates, $D_{Y,\xi}(U_n) = \hat{H}_Y^{-1}(S_\xi(U_n))$, will still have marginal distribution $\hat{H}_Y$, while the corresponding sample paths will be ξ-skewed.

Figure 4 displays a typical cyclical sample path before and after stitching. Specifically, Figure 4(a) was generated by an unstitched basic ARM$^+$ sequence, $\{U_n^+\}$, with an innovation of the form (8) and parameters $(\alpha, \phi) = (0.1, 0.5)$, whereas Figure 4(b) displays a sample path of the stitched process, $\{S_\xi(U_n^+)\}$, with stitching parameter $\xi = 0.5$. Note how
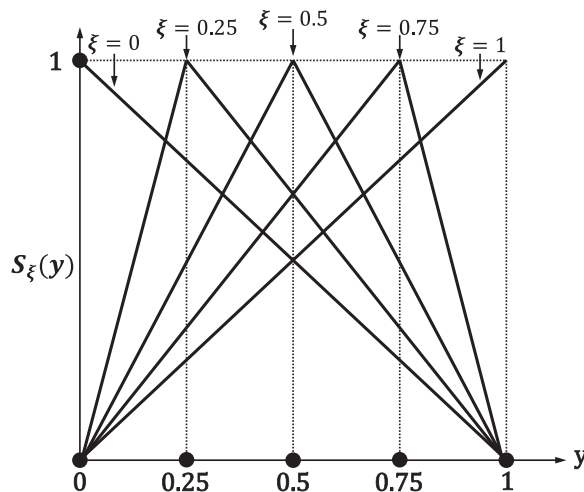

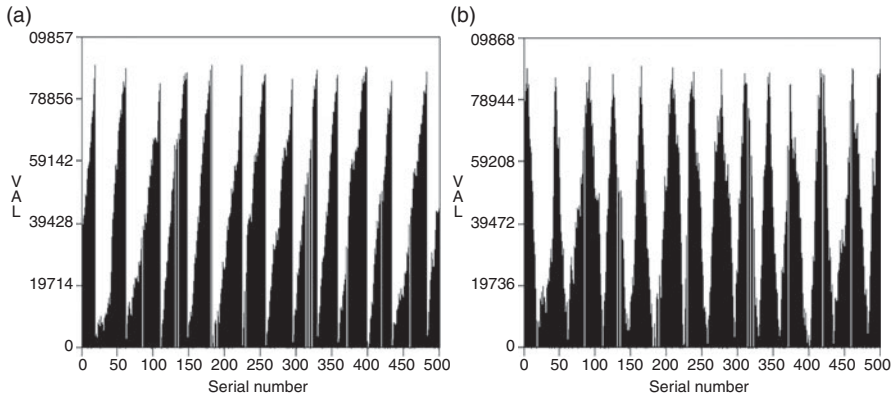FIGURE 3. Examples of stitching transformations.

FIGURE **4.** Cyclical sample paths from a basic ARM$^+$ process ($\alpha = 0.1, \phi = 0.5$) before and after stitching. (a) Unstitched sample path ($\xi = 1$). (b) Stitched sample path ($\xi = 0.5$).

the sawtooth cycles changed to symmetric (zero skew) cycles, even though the marginal distribution corresponding to both paths is still uniform on $[0, 1)$. It can be shown that for an ARM background sequence, decreasing ξ in the interval $[0, 0.5]$ or increasing ξ in the interval $[0.5, 1]$ results in new sequences whose autocorrelation magnitudes are strictly monotonically decreasing. The highest magnitude occurs for $\xi = 0.5$. Interestingly, the autocorrelation functions of $\{S_\xi(U_n^+)\}$ and $\{S_{1-\xi}(U_n^+)\}$ are identical, though the corresponding sample paths have skews ξ and $1 - \xi$, respectively.

4.2. Distribution-Invariant Operators

In this section, we exhibit a number of operators that map an inverse histogram distortion, $\hat{H}_Y^{-1}$, to piecewise-linear distortions such that the resulting foreground sequence retains the prescribed histogram cdf, $\hat{H}_Y$. More generally, a transformation $\mathcal{F}$ of a distortion D is called a *distribution-invariant operator*, provided the random variables, $D[U]$ and $\mathcal{F}[D](U)$, have the same distribution. Here, we shall restrict attention to piecewise-linear distortions – not necessarily monotone – of which $\hat{H}_Y^{-1}$ is a special (monotone) case.

The graph of a piecewise-linear distortion, L, can be specified by a collection of line segments connecting pairs of two-dimensional points (see, e.g., Figure 2(b)). To put things in the inverse histogram distortion context of Section 3, we shall assume the following setup for a piecewise-linear distortion, L. Let $\{p_j\}_{j=1}^J$ be a discrete pdf with a corresponding cdf $\{C_j\}_{j=0}^J$, where $C_0 = 0, C_j = \sum_{i=1}^j p_i$ for $1 \le j \le J$, and $C_J = 1$. Then a tuple of the form $(C_{j-1}, s_{j-1}, C_j, s_j)$ is called a *linear component* of L, provided the line segment connecting point (C_{j-1}, s_{j-1}) to point (C_j, s_j) in the two-dimensional plane, is a restriction of the graph of L.

Note that an inverse histogram distortion, $\hat{H}_Y^{-1}$, is always monotonically increasing, since each of its components is. However, the distortion D obtained by applying a series of distribution-invariant operators (to be defined in the sequel) may not necessarily be monotone, as its components may be either monotonically increasing or monotonically decreasing. In order to capture this mixed behavior, we generalize in the remainder of the paper the quantity $w_j = s_j - s_{j-1}$ by allowing it to assume either positive values (on monotonically increasing components) or negative values (on monotonically decreasing components).

We now proceed to present four classes of elementary distribution-invariant operators, which map piecewise-linear distortions to piecewise-linear distortions with the same support. Their effects will be illustrated on the linear distortion function of Figure 2(b).
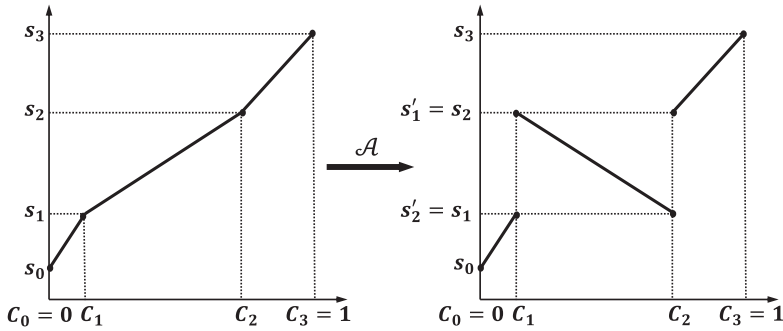
FIGURE **5.** Example of operator $\mathcal{A}$.

4.2.1. Operator $\mathcal{A}$ (antithetic distortion components). Let $(C_{j-1}, s_{j-1}, C_j, s_j)$ be any linear component of L. The effect of the operator $\mathcal{A}$ is to replace $(C_{j-1}, s_{j-1}, C_j, s_j)$ by the linear component $(C_{j-1}, s'_{j-1}, C_j, s'_j) = (C_{j-1}, s_j, C_j, s_{j-1})$. Figure 5 illustrates the effect of the operator $\mathcal{A}$ on the middle linear component of Figure 2(b). Clearly, $\mathcal{A}[L]$ is a linear distortion with the same support as L. To see that $\mathcal{A}$ also preserves the marginal distribution of $L(U)$, note first that on the event $\{U \in [C_{j-1}, C_j]\}$, one has

$$L(U) = s_{j-1} + (U - C_{j-1})\frac{w_j}{p_j}, \quad \mathcal{A}[L](U) = s_j + (U - C_{j-1})\frac{w'_j}{p_j},$$

where $w'_j = s'_j - s'_{j-1} = s_{j-1} - s_j < 0$. Thus, on $U \in [C_{j-1}, C_j]$, each of the variates $L(U)$ and $\mathcal{A}[L](U)$ is distributed uniformly on $[s_{j-1}, s_j]$; in fact, in this case, $\mathcal{A}[L](U)$ is the antithetic version of $L(U)$. It follows that both variates, $L(U)$ and $\mathcal{A}[L](U)$, have the same distribution.

4.2.2. Operator $\mathcal{P}$ (permutation of distortion components). Let $(C_{m-1}, s_{m-1}, C_m, s_m)$ and $(C_{n-1}, s_{n-1}, C_n, s_n)$ be any two distinct linear components of L. The effect of the operator $\mathcal{P}$ is to permute (interchange) the two linear components in the following way. First interchange the indices of p_m and p_n, yielding a new discrete pdf $\{p'_j\}_{j=1}^J$, where $p'_m = p_n$, $p'_n = p_m$, and $p'_j = p_j$ for all other j; the new $\{p'_j\}_{j=1}^J$ induces a new cdf, $\{C'_j\}_{j=0}^J$, where $C'_j = \sum_{i=1}^j p'_i$. And second, interchange similarly, s_{m-1} with s_{n-1} and s_m with s_n, yielding new sequences $\{s'_j\}$.

Figure 6 illustrates the effect of the operator $\mathcal{P}$ on the first and third linear components of Figure 2(b). Clearly, $\mathcal{P}[L]$ is a linear distortion with the same support as L. To see that $\mathcal{P}$ also preserves the marginal distribution of $L(U)$, note that the probabilities $P\{U \in [C'_{j-1}, C'_j]\}$ constitute a mere relabeling, relative to those in L, and that the conditional probabilities of sampling a value of $\mathcal{P}[L](U)$ in an interval $[s_{j-1}, s_j)$ are unchanged. It follows that both variates, $L(U)$ and $\mathcal{P}[L](U)$, have the same distribution.

4.2.3. Operator $\mathcal{S}$ (splitting of distortion components). Let $(C_{j-1}, s_{j-1}, C_j, s_j)$ be a linear component of L. The effect of the operator $\mathcal{S}$ is to split $(C_{j-1}, s_{j-1}, C_j, s_j)$ into two contiguous linear components as follows. First, split the probability p_j into a sum, $p_j = p'_j + p''_j$, where $p'_j > 0$ and $p''_j > 0$. Next, define $C'_{j-1} \in [C_{j-1}, C_j)$, by $C'_{j-1} = C_{j-1} + p'_j$. Now replace the original linear component, $(C_{j-1}, s_{j-1}, C_j, s_j)$, by the two linear components: $(C_{j-1}, s_{j-1}, C'_{j-1}, s_j)$ and $(C'_{j-1}, s_{j-1}, C_j, s_j)$. In effect, if we view $\{C_j\}_{j=1}^J$ as a
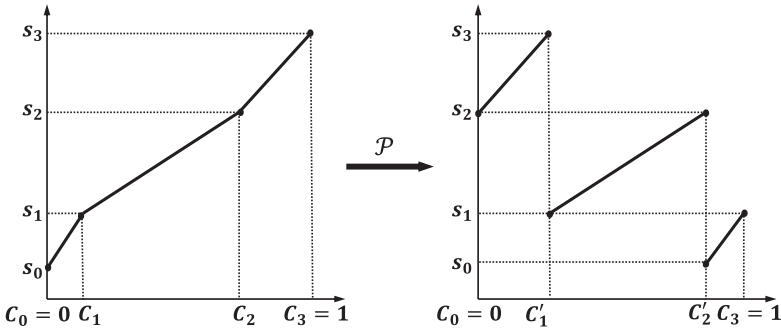
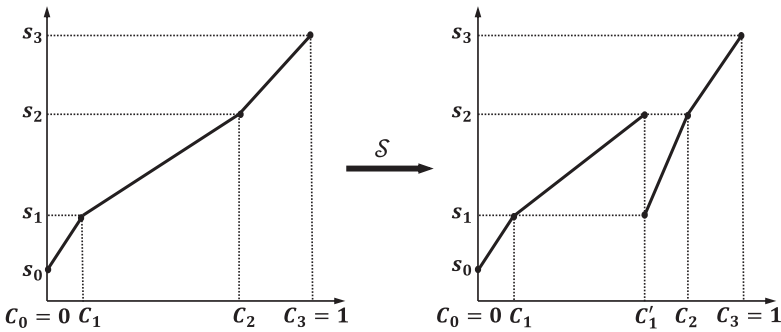FIGURE **6.** Example of operator $\mathcal{P}$.

FIGURE **7.** Example of operator $\mathcal{S}$.

partition of the interval $[0, 1)$, then the effect of $\mathcal{S}$ is to refine that partition by adding the point $C'_{j-1} = C_{j-1} + p'_j$ in the interval $[C_{j-1}, C_j)$.

Figure 7 illustrates the effect of the operator $\mathcal{S}$ on the middle linear component of Figure 2(b). Clearly, $\mathcal{S}[L]$ is a linear distortion with the same support as L. To see that $\mathcal{S}$ also preserves the marginal distribution of $L(U)$, note that

$$P\{U \in [C_{j-1}, C'_{j-1}) \cup [C'_{j-1}, C_j)\} = p'_j + p''_j = p_j,$$

and that conditional on either $\{U \in [C_{j-1}, C'_{j-1})\}$ or $\{U \in [C'_{j-1}, C_j)\}$, $S[L](U)$ is uniform on $[s_{j-1}, s_j)$, whereas all other probabilities are unchanged. It follows that both $L(U)$ and $S[L](U)$ have the same distribution.

4.2.4. Operator $\mathcal{N}$ (nominal splitting of distortion components). Let $(C_{j-1}, s_{j-1}, C_j, s_j)$ be a linear component of L. The effect of the operator $\mathcal{N}$ is to split $(C_{j-1}, s_{j-1}, C_j, s_j)$ into two contiguous linear components, but unlike the $\mathcal{S}$ operator, the split is only nominal in the sense that $L(U)$ and $\mathcal{S}[L](U)$ are identical distortions. Specifically, we again split p_j into a sum $p_j = p'_j + p''_j$ as before, letting $C'_{j-1} = C_{j-1} + p'_j$ as above. We further define $s'_{j-1} \in [s_{j-1}, s_j)$ by $s'_{j-1} = s_{j-1} + (s_j - s_{j-1})(p'_j/p_j)$. Now replace the original linear component, $(C_{j-1}, s_{j-1}, C_j, s_j)$, by the two linear components, $(C_{j-1}, s_{j-1}, C'_{j-1}, s'_{j-1})$ and $(C'_{j-1}, s'_{j-1}, C_j, s_j)$.

Figure 8 illustrates the effect of the operator $\mathcal{N}$ on the middle linear component of Figure 2(b). Note that the two new linear components represent line segments that are juxtaposed "seamlessly", effectively rendering $\mathcal{N}$ an identity operator. However, the merit of replacing a linear component by two equivalent ones is an added flexibility, since all the
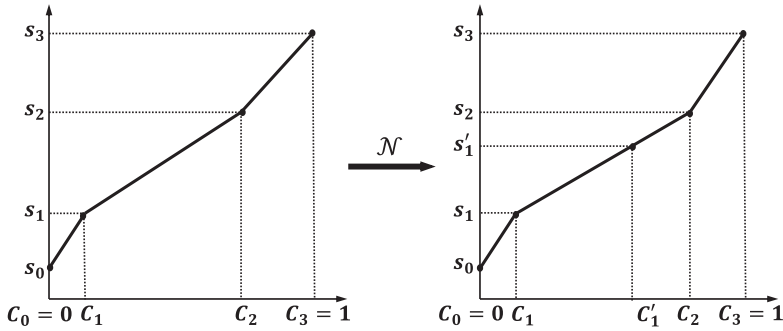
FIGURE **8.** Example of operator $\mathcal{N}$.

previous operators can still be applied to each of the new linear components, and therefore, to subsets of $(C_{j-1}, s_{j-1}, C_j, s_j)$.

5. TEMPORAL SHAPING OF TIME SERIES

In this section, we put all pieces together to propose a heuristic procedure for temporal shaping of time series. Assuming that the cycle profile has already been normalized as per Eq. (6), the temporal shaping procedure consists of two steps:

1. *Profile shaping*: In this step, we use a heuristic procedure (typically with human interaction) that applies a sequence of distribution-invariant operators, defined in Section 4.2, to the prescribed inverse histogram distortion, $\hat{H}_Y^{-1}$, with the goal of constructing a distortion, D, which approximates the prescribed cycle profile. Recall that such a distortion preserves the prescribed marginal histogram cdf, $\hat{H}_Y$.

2. *Autocorrelation approximation*: In this step, we employ a search algorithm, which uses the distortion D obtained in the previous step, and searches for innovation and stitching parameters, which jointly define an ARM model that approximates the prescribed autocorrelation function and simultaneously preserves the prescribed marginal histogram cdf, $\hat{H}_Y$.

5.1. Heuristic Procedure for Profile Shaping

Let $\mathcal{C}(L)$ denote the *closure set* of a piecewise-linear distortion L, obtained by applying to L all possible sequences of the distribution-invariant operators, $\mathcal{A}$, $\mathcal{P}$, $\mathcal{S}$, and $\mathcal{N}$. The application of stitching transformations composed with such operators is also permissible.

Note that while distortion elements of a closure set give rise to foreground sequences with the same marginal distribution as $L(U)$, they are not necessarily monotone distortions. The basic idea of the heuristic temporal shaping is to search a closure set for an appropriate distortion.

Consider now the special case of an inverse histogram distortion, namely, $L = \hat{H}_Y^{-1}$. For each cell $(s_{j-1}, s_j, \hat{p}_j)$ in the underlying histogram, $\hat{\mathcal{H}}_Y$, there is a corresponding linear component, $(\hat{C}_{j-1}, s_{j-1}, \hat{C}_j, s_j)$ of $\hat{H}_Y^{-1}$. In this case, the heuristic temporal shaping procedure is concerned with the closure set $\mathcal{C}(\hat{H}_Y^{-1})$. Specifically, assume that a cycle "profile" is prescribed as a normalized curve over the domain $[0, 1)$. The goal is to start with $\hat{H}_Y^{-1}$, which is a non-decreasing piecewise-linear distortion, and proceed to apply to it distribution-invariant

operators, so as to roughly fit the prescribed cycle profile. In effect, the heuristic search procedure searches along trajectories of linear distortions in the closure set $\mathcal{C}(\hat{H}_Y^{-1})$, starting with the initial $\hat{H}_Y^{-1}$. That each distortion encountered preserves the cdf $\hat{H}_Y$, is guaranteed by the discussion in the previous sections. Ultimately, we seek a piecewise-linear distortion $D \in \mathcal{C}(\hat{H}_Y^{-1})$, such that $D(U_n)$ approximates the cyclical structure of $\{Y_n\}$. Recall that $\{U_n\}$ is a positively autocorrelated process with the Uniform (0,1) marginal distribution, playing the role of pseudo-time within sample path cycles.

From a visual point of view, the heuristic search activity amounts to "chopping up" $\hat{H}_Y^{-1}$ into linear components (possibly adding new ones or eliminating old ones), and then reassembling the pieces into an acceptable fit of the prescribed profile. Figure 9 shows an example of such fitting. The left-hand side graph depicts an inverse histogram distribution (dashed curve) superimposed on some prescribed profile (solid curve). The right-hand side graph depicts the same profile (solid curve) superimposed on the piecewise-linear distortion (dashed curve) obtained as a result of a fitting session. To simplify notation, linear components will be referred to through their domains: $[C_{j-1}, C_j)$ will denote a generic linear component in the left-hand side graph, while $[C'_{j-1}, C'_j)$ will denote the same in the right-hand side graph. With these notational conventions, the transformations applied in Figure 9 are as follows.

1. The linear component $[C_0, C_1)$ was split into two pieces by an $\mathcal{S}$ operator. The first piece, $[C'_0, C'_1)$, stayed in place, while the second piece was rendered antithetic (descending) by an $\mathcal{A}$ operator and then permuted by a $\mathcal{P}$ operator, ending up as the rightmost linear component, $[C'_5, C'_6)$.

2. The linear component $[C_1, C_2)$ was first split by an $\mathcal{S}$ operator and both pieces were permuted away from their position, ending up as linear components $[C'_1, C'_2)$ and $[C'_4, C'_5]$. The latter was rendered antithetic by an $\mathcal{A}$ operator.

3. The linear component $[C_2, C_3)$ was manipulated similarly to the previous one, ending up as linear components $[C'_2, C'_3)$ and $[C'_3, C'_4)$.

We point out that the fitting performed in Figure 9 is just one among many alternatives. However, the common pattern of such fittings is apparent: the linear components of the (monotone) inverse histogram distortion are split up by $\mathcal{S}$ operators and usually permuted away from their current position by $\mathcal{P}$ operators to fit one ascending portion and one descending portion of the prescribed cycle profile, the latter via $\mathcal{A}$ operators. If the profile is not symmetric, in the sense that the cycle profile does not terminate at its initial point, then $\mathcal{N}$ operators may be used in lieu of $\mathcal{S}$ operators to capture such asymmetries.
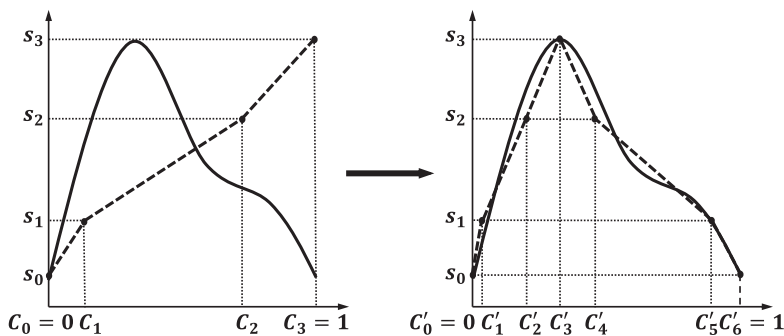

FIGURE **9.** Example of shaping an inverse histogram to comport with a prescribed profile.

5.2. Autocorrelation Approximation

Given the distortion D, obtained by shaping the profile using distribution-invariant operators, the next step is to search for innovation and stitching parameters that give rise to an ARM model which approximates the prescribed autocorrelation function while preserving the prescribed marginal histogram cdf, $\mathcal{H}_Y$. Essentially, we seek an optimal pair of innovation density and stitching parameter (f_V^*, ξ^*), such that the weighted sum of squared differences between the empirical and modeled autocorrelations is minimized, that is,

$$(f_V^*, \xi^*) = \underset{(f_V, \xi)}{\operatorname{argmin}} \left\{ \sum_{\tau=1}^{T} a_\tau [\rho_{f_V, \xi}(\tau) - \hat{\rho}_Y(\tau)]^2 \right\}, \tag{10}$$

where T is the maximal autocorrelation lag to be approximated, a_τ $(0 < a_\tau \le 1)$ is a weight coefficient for the term corresponding to lag τ, and $\rho_{f_V, \xi}(\tau)$ is the model autocorrelation of lag τ. To this end, we employ a variant of a heuristic search algorithm, called global search local optimization (GSLO) (Jagerman and Melamed [11]; Jelenkovic and Melamed [12,13]), adapted to basic ARM$^+$ processes with uniform innovations of the form (8), to be reviewed next.

The lag τ autocorrelation of an ARM$^+$ process $\{X_n\}$ is given by (Jelenkovic and Melamed [13])

$$\rho_{f_V, \xi}(\tau) = \frac{2}{\sigma_X^2} \sum_{\nu=1}^{\infty} \operatorname{Re}[\tilde{f}_V^\tau(i2\pi\nu)] |\tilde{D}_\xi(i2\pi\nu)|^2, \tag{11}$$

where $0 < \sigma_X^2 < \infty$ is the common variance of $\{X_n\}$, $\tilde{f}_V$ is the Laplace transform of innovation f_V, and $\tilde{D}_\xi$ is the Laplace transform of distortion D composed with stitching transformation S_ξ. In particular, for a uniform innovation of the form (8), Proposition 1 in Jagerman and Melamed [9] has

$$\operatorname{Re}\left[\tilde{f}_V^\tau(i2\pi\nu)\right] = \cos(\pi\nu(R+L)\tau) \left(\frac{\sin(\pi\nu(R-L))}{\pi\nu(R-L)}\right)^\tau. \tag{12}$$

Furthermore, for the piecewise-linear distortions of Section 5.1, Jagerman and Melamed [9], (Proposition 4) has

$$\left|\tilde{D}_\xi(i2\pi\nu)\right|^2 = a_{\xi,\nu}^2 + b_{\xi,\nu}^2, \tag{13}$$

where

$$\begin{aligned}
a_{\xi,\nu} = &\sum_{j=1}^{J} \frac{s_j[\sin(2\pi\nu\xi C_j) + \sin(2\pi\nu(1-\xi)C_j)]}{2\pi\nu} \\
&- \sum_{j=1}^{J} \frac{s_{j-1}[\sin(2\pi\nu\xi C_{j-1}) + \sin(2\pi\nu(1-\xi)C_{j-1})]}{2\pi\nu} \\
&+ \sum_{j=1}^{J} \frac{w_j}{p_j} \frac{\cos(2\pi\nu\xi C_j) - \cos(2\pi\nu\xi C_{j-1})}{\xi(2\pi\nu)^2} \\
&+ \sum_{j=1}^{J} \frac{w_j}{p_j} \frac{\cos(2\pi\nu(1-\xi)C_j) - \cos(2\pi\nu(1-\xi)C_{j-1})}{(1-\xi)(2\pi\nu)^2},
\end{aligned} \tag{14}$$

$$b_{\xi,\nu} = \sum_{j=1}^{J} \frac{s_j[\cos(2\pi\nu\xi C_j) - \cos(2\pi\nu(1-\xi)C_j)]}{2\pi\nu}$$

$$- \sum_{j=1}^{J} \frac{s_{j-1}[\cos(2\pi\nu\xi C_{j-1}) - \cos(2\pi\nu(1-\xi)C_{j-1})]}{2\pi\nu}$$

$$- \sum_{j=1}^{J} \frac{w_j}{p_j} \frac{\sin(2\pi\nu\xi C_j) - \sin(2\pi\nu\xi C_{j-1})}{\xi(2\pi\nu)^2}$$

$$+ \sum_{j=1}^{J} \frac{w_j}{p_j} \frac{\sin(2\pi\nu(1-\xi)C_j) - \sin(2\pi\nu(1-\xi)C_{j-1})}{(1-\xi)(2\pi\nu)^2}. \qquad \textbf{(15)}$$

We mention that the results in Eqs. (14) and (15) were previously derived in Jagerman and Melamed [9] for piecewise-linear and monotonically increasing distortions (cf. ibid., Eqs. (3.7) and (3.8)); however, they actually extend to any piecewise-linear distortions, provided we admit negative-valued w_j for each portion of D that decreases monotonically over the associated interval $[C_{j-1}, C_j]$. The derivation of Eqs. (14) and (15) is identical to its counterpart in Jagerman and Melamed [9].

Next, substituting (12) and (13) into (11), we have in our case,

$$\rho_{R,L,\xi}(\tau) = \frac{2}{\sigma_X^2} \sum_{\nu=1}^{\infty} \cos\left(\pi\nu(R+L)\tau\right) \left(\frac{\sin\left(\pi\nu(R-L)\right)}{\pi\nu(R-L)}\right)^{\tau} (a_{\xi,\nu}^2 + b_{\xi,\nu}^2), \qquad \textbf{(16)}$$

where $a_{\xi,\nu}$ and $b_{\xi,\nu}$ are given by Eqs. (14) and (15), respectively. Partial derivatives of $\rho_{R,L,\xi}(\tau)$ with respect to R, L, and ξ are computed from Eq. (16) (see Jelenkovic and Melamed [13]), and will not be reproduced here.

In our case, we search for an optimal triple (R^*, L^*, ξ^*) in the following non-linear optimization problem:

$$\min_{(R,L,\xi)} \sum_{\tau=1}^{T} a_\tau [\rho_{R,L,\xi}(\tau) - \hat{\rho}_Y(\tau)]^2,$$

$$\text{s.t.} -0.5 \le L < R < 0.5,$$

$$0 \le \xi \le 1.$$

To this end, we implement a variant of the GSLO algorithm, modified to take advantage of the simpler structure of the abovementioned optimization problem. This algorithm consists of three steps: it first discretizes the solution space by partitioning it into equal-size cubes; then explores the neighborhood of each cube's center by a Steepest Descent algorithm for a locally optimal solution; and finally selects a near-optimal solution as the best of all locally optimal solutions. More specifically, the proposed algorithm (to be referred to as *Simplified GSLO*) unfolds as follows:

1. Divide the solution space into equal-size cubes with centers

$$(L, R, \xi) = \left(-0.5 + \frac{2m+1}{2K}, -0.5 + \frac{2n+1}{2K}, \frac{2l+1}{2K}\right),$$

where K, m, n, and l are integers, such that $0 \le m < n \le K-1$, and $0 \le l \le K-1$.

2. Starting from each of the center points above, use the Frank–Wolfe algorithm
   (Bertsekas [1], p. 215) to solve the following non-linear optimization problem,

$$\min_{(R,L,\xi)} \sum_{\tau=1}^{T} a_\tau [\rho_{R,L,\xi}(\tau) - \hat{\rho}_Y(\tau)]^2,$$

$$\text{s.t.} \ -0.5 + \frac{m}{K} \leq L < -0.5 + \frac{m+1}{K},$$

$$-0.5 + \frac{n}{K} \leq R < -0.5 + \frac{n+1}{K},$$

$$\frac{l}{K} \leq \xi \leq \frac{l+1}{K}.$$

3. Select the minimal solution from the set obtained in step 2.

5.3. Numerical Example

To test the performance of the proposed temporal shaping algorithm, we analyzed an empirical time series $\{y_n\}$, consisting of 1,000 equal-length cycles of 25 (random) observations for a total of 25,000 observations. The initial portion of the $\{y_n\}$ time series and the associated histogram pdf and cdf of the entire $\{y_n\}$ time series are shown in Figure 10.

A non-normalized cycle profile was constructed from the aforementioned empirical time series by averaging all points in the same cycle position, and then normalized as per Eq. (6). Figure 11(a) depicts the profile (solid curve) with the inverse histogram (dotted line) corresponding to the cdf in Figure 10(c). We then shaped the inverse histogram of Figure 11(a) to comport with that profile by applying heuristically the distribution-invariant operators as described in Section 5.1, with the result shown in Figure 11(b).

Next, we set $T = 10$, $a_\tau = 1$ for all $\tau = 1, \ldots, T$ and $K = 20$, and ran the Simplified GSLO algorithm to find the optimal innovation and stitching parameter for two ARM models, $\{X_n^1\}$ and $\{X_n^2\}$, using respectively the distortion with the inverse histogram in Figure 11(a) and the shaped inverse histogram in Figure 11(b). Finally, we generated 100 sample paths using each of the models, $\{X_n^1\}$ and $\{X_n^2\}$.

Figure 12(a) compares the histogram pdf of $\{y_n\}$ (solid curve) to the histogram pdfs selected randomly from the 100 sample paths generated by the ARM models $\{X_n^1\}$ and $\{X_n^2\}$ (dashed and dotted curves, respectively). The agreement among those three histograms confirms that both $\{X_n^1\}$ and $\{X_n^2\}$ preserve the distribution of the empirical time series, $\{y_n\}$. Figure 12(b) further depicts the initial portion of the corresponding three sample paths. It shows that the sample path generated by the model $\{X_n^2\}$ using the shaped inverse histogram (dotted curve) better matches the empirical time series $\{y_n\}$ (solid curve) and its cyclical pattern than its $\{X_n^1\}$ counterpart (dashed curve).

Finally, we computed the autocorrelation functions of lag $\tau = 1, \ldots, T$, for $\{y_n\}$ and the 100 sample paths generated by each of $\{X_n^1\}$ and $\{X_n^2\}$. Figure 13(a) compares the autocorrelation function of $\{y_n\}$ (solid line) to the average autocorrelations, averaged over the respective 100 sample paths generated by $\{X_n^1\}$ (circles) and $\{X_n^2\}$ (squares). It shows that both models approximate the empirical autocorrelations closely. Figure 13(b) further shows the *total autocorrelations discrepancy* as the weighted sums of squared differences between the empirical and modeled autocorrelations ($\sum_{\tau=1}^{T} a_\tau [\hat{\rho}_X(\tau) - \hat{\rho}_Y(\tau)]^2$) for each sample path generated by $\{X_n^1\}$ and $\{X_n^2\}$. It is observed that the model $\{X_n^2\}$ using the shaped inverse histogram improves the approximation of autocorrelations, as compared to the model $\{X_n^1\}$. The improvement averages about 41%.
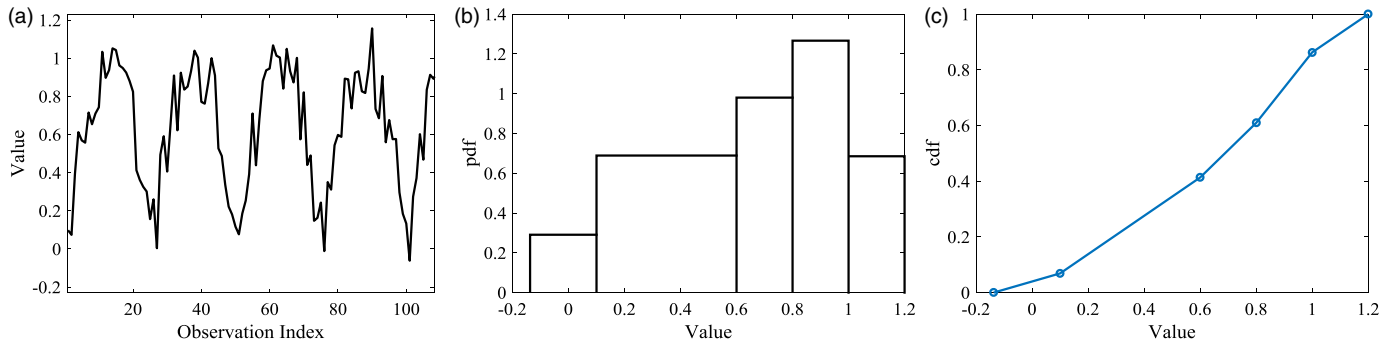
FIGURE **10.** Empirical statistics of the time series $\{y_n\}$. (a) Initial portion of $\{y_n\}$. (b) Histogram pdf of $\{y_n\}$. (c) Corresponding cdf of $\{y_n\}$.
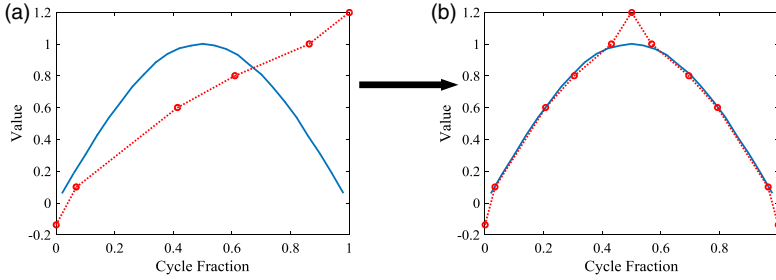
FIGURE **11.** Shaping an inverse histogram to comport with the cycle profile of $\{y_n\}$. (a) Cycle profile and the inverse histogram to be shaped. (b) Cycle profile and the shaped inverse histogram.
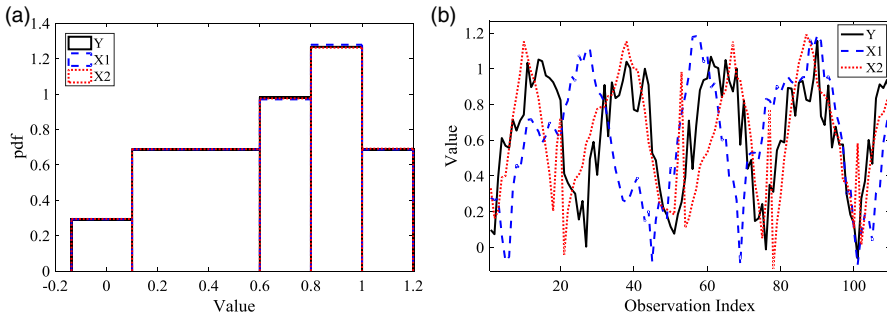

FIGURE **12.** Comparisons of histograms and sample paths of $\{Y_n\}$, $\{X_n^1\}$, and $\{X_n^2\}$. (a) Comparison of histogram pdfs. (b) Comparison of sample paths.
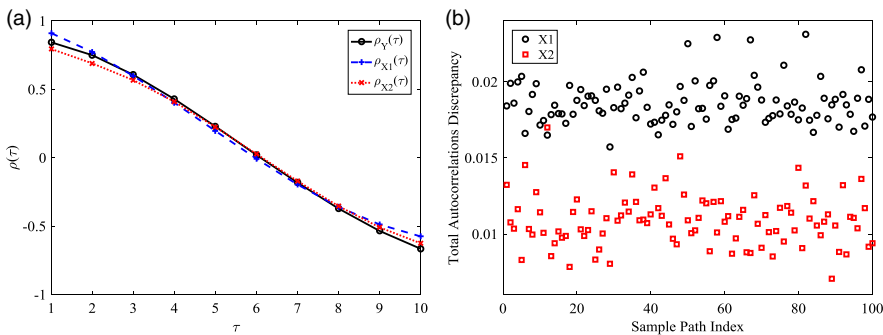

FIGURE **13.** Comparisons of autocorrelations. (a) Comparison of the autocorrelation functions. (b) Comparison of total autocorrelations discrepancies.

The numerical examples demonstrate that the proposed temporal shaping method is capable of generating sample paths that match the empirical marginal distribution and closely approximate the empirical autocorrelation function.

6. CONCLUSION

We have introduced the concept of temporal shaping in the context of Monte Carlo simulation modeling of cyclical stationary time series, utilizing the inversion method. The goal of temporal shaping is to give rise to simulated sample paths that "conform" to a prescribed cycle profile, while retaining the empirical distribution. Such "conformity" also tends to improve the fit of the model autocorrelation function to its empirical counterpart.

Finally, we observe that since the heuristic shaping activity is inherently visual and interactive in nature, it is reasonable to suggest that it would be effectively carried out with the aid of software. It may also be possible to use expert-system technology to perform automated heuristic searches to assist a human worker in manual searches.

References

1. Bertsekas, D.P. (1999). *Nonlinear programming*, 2nd ed. Athena Scientific, Belmont, Massachusetts, USA.
2. Bratley, P., Fox, B.L., & Schrage, L.E. (1987). *A guide to simulation*. Springer-Verlag, New York, NY, USA.
3. Cario, M.C. & Nelson, B.L. (1996). Autoregressive to anything: Time-series input processes for simulation. *OR Letters* 19: 51–58.
4. Cario, M.C. & Nelson, B.L. (1998). Numerical methods for fitting and simulating autoregressive-to-anything processes. *INFORMS Journal on Computing* 10(1): 72–81.
5. Feller, W. (1971). *An introduction to probability theory and its applications*, vol. 2, 2nd ed. John Wiley & Sons, Inc., New York, NY, USA.
6. Liu, B. & Munson, D.C. (1982). Generation of a random sequence having a jointly specified marginal distribution and autocovariance. *IEEE Transactions on Acoustics, Speech and Signal Processing* 30(6): 973–983.
7. Lewis, P.A.W. & McKenzie, E. (1991). Minification processes and their transformations. *Journal of Applied Probability* 28: 45–57.
8. Jagerman, D.L. & Melamed, B. (1992). The transition and autocorrelation structure of TES processes part I: General theory. *Stochastic Models* 8(2): 193–219.
9. Jagerman, D.L. & Melamed, B. (1992). The transition and autocorrelation structure of TES processes part II: Special cases. *Stochastic Models* 8(3): 499–527.
10. Jagerman, D.L. & Melamed, B. (1994). The spectral structure of TES processes. *Stochastic Models* 10(3): 599–618.
11. Jagerman, D.L. & Melamed, B. (1995). Bidirectional estimation and confidence regions for TES processes. *Proceedings of MASCOTS '95*, Durham, North Carolina, pp. 94–98.
12. Jelenkovic, P. & Melamed, B. (1995). Automated TES modeling of compressed video. *Proceedings of IEEE INFOCOM '95*, Boston, Massachusetts, pp. 746–752.
13. Jelenkovic, P. & Melamed, B. (1995). Algorithmic modeling of TES processes. *IEEE Transactions on Automatic Control* 40(7): 1305–1312.
14. Melamed, B. (1991). TES: A class of methods for generating autocorrelated uniform variates. *ORSA Journal on Computing* 3(4): 317–329.
15. Melamed, B. (1993). An overview of TES processes and modeling methodology. In L. Donatiello & R. Nelson (eds.), *Performance evaluation of computer and communications systems*. Springer-Verlag Berlin Heidelberg Lecture Notes in Computer Science, pp. 359–393.
16. Melamed, B. (1999). ARM processes and modeling methodology. *Stochastic Models* 15(5): 903–929.